Range and Velocity Estimations in Multi-band Hybrid Multistatic Radar Networks

Murat Temiz[1] , Hugh Griffiths[1], Matthew Ritchie[1]*

[1]*Department of Electronic and Electrical Engineering, University College London, London, United Kingdom*
**E-mail: m.temiz@ucl.ac.uk*

Keywords: Multistatic Radar, Passive Radar, Multiwaveform Radar Sensing, Range and Velocity Estimations

Abstract

This study investigates the benefits of exploiting multiple illuminators of opportunity (IOs) in hybrid radar systems consisting of multi-band receivers that can utilise active radar waveforms and broadcasting signals for multistatic radar sensing. As a performance metric, Cramér-Rao lower bounds (CRLBs) on the range and velocity estimations are considered. FM radio, Digital Video Broadcasting-Terrestrial (DVB-T) and Digital Audio Broadcasting (DAB) transmitters are considered as IOs for passive radar sensing while also having an active radar transmitter in the multistatic radar network. The multistatic radar networks consisting of receivers, transmitters and IOs are modelled and simulated and CRLBs on the range and velocity estimations are calculated. Two different multistatic radar network scenarios are simulated and the results are evaluated to analyse the estimation accuracy of active and passive bistatic pairs. The results show that a multi-band multistatic radar network can provide better range and velocity estimations by exploiting IO signals compared to a radar network that only uses traditional active radar waveforms.

1 Introduction

Passive radar systems make use of broadcasting, communication or radio navigation transmissions as illuminators of opportunity (IOs) for target detection instead of having dedicated radar transmitters [1]. Passive radar is also known as passive bistatic radar (PBR) since the broadcasting stations and receivers can be in different locations [2]. PBR is especially attractive for stealth and low-cost sensing or experimental research since it does not require any transmitter (Tx), hence only a receiver (Rx) equipped with surveillance and reference antennas is sufficient for radar measurements. However, broadcasting or communication signals are not specifically designed for radar sensing and their properties vary over time depending on the data transmitted, hence this affects the sensing performance. Moreover, the bistatic geometry between the Tx-target-Rx pairs significantly impacts the accuracy of target detection and parameter estimations. Therefore, the geometry of the bistatic Tx-Rx pairs must be considered in addition to waveform parameters and received signal power while evaluating the performance of multistatic radar systems [3]. Various broadcasting or communication signals have been considered as IOs for passive radar sensing. Among these, FM radio, DVB-T, and DAB signals are desirable ones for long-range sensing applications due to their wide area coverage, high transmit power, sufficient bandwidth and well-known waveform structures [4].

In this study, we consider a hybrid multi-band multistatic radar network consisting of a radar transmitter and also utilises IOs available in the area of interest to enhance the target parameter estimations. As the bistatic geometry significantly impacts the parameter estimation, the optimum Tx-Rx pair for achieving the best estimation accuracy chiefly depends on the location of the target [5]. Consequently, although active radar sensing is expected to outperform passive radar sensing in most cases, passive bistatic pairs may perform better for some specific target locations depending on the bistatic geometry and signal-to-noise ratio (SNR) or signal-to-interference-plus-noise ratio (SINR). Moreover, the radar system may want to switch off its active transmitter to reduce its detectability. In order to make this decision, the knowledge of active radar performance versus passive radar performance is required. Therefore, the purpose of this study is to investigate the theoretical performance of multi-waveform hybrid multistatic radar networks.

Cramér–Rao lower bounds (CRLBs) have been widely used in radar studies to evaluate the performance of various radar systems and waveforms, and also used as a benchmark for estimation algorithms as it defines the lower bounds of mean squared error (MSE) of the estimation for unbiased estimators. [6]. Efficient unbiased estimators can attain CRLBs, for instance, the maximum likelihood estimator (MLE) was shown to reach the CRLBs when the received radar returns have sufficient SNR [7]. Therefore, CRLBs on the range and velocity estimations are used as performance metrics to evaluate the performance of Tx-Rx pairs in this study. While CRLBs on target parameter estimations are functions of only SNR (or SINR) and radar waveform in monostatic radar systems [8], bistatic geometry has a significant impact on the CRLBs in bistatic radar networks [5].

This study considers multiple waveforms transmitted by different broadcasting systems possibly available in the area of interest to improve the range and velocity estimations. Multi-band receivers equipped with multiple surveillance and reference antennas are used to perform both passive and active radar sensing. Such multi-band multi-waveform passive radar

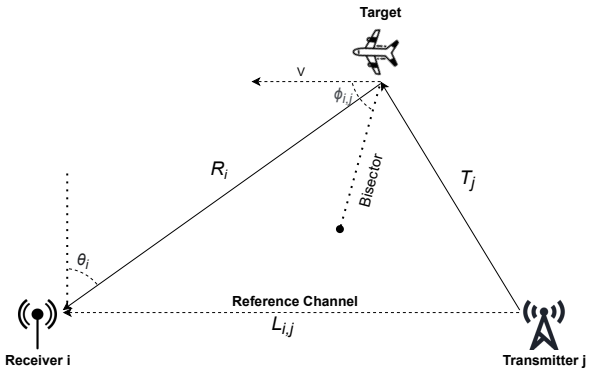

Fig. 1 Bistatic geometry between the jth Tx, target and ith Rx.

receivers have already been developed, implemented and measured to evaluate their performance in [9, 10], which demonstrated that FM radio, DAB, and DVB-T signals can be jointly and efficiently utilised for passive radar sensing. There are significant advantages of utilising multiple IOs operating at different frequency bands. Firstly, utilising different frequencies and IO signals in addition to active radar sensing results in a substantially more robust radar system against any potential jamming since multi-band jamming is not an easy task and the jammer probably does not know which frequencies are used for passive sensing [11]. Secondly, the radar transmitter may be switched off anytime to enable passive sensing by jointly utilising IOs. Thirdly, as the IOs are distributed in the area, the impact of bistatic geometry on the radar sensing may be mitigated by selecting optimum Tx-Rx pairs for different target locations [12]. In addition to utilising multiple IO waveforms, we also consider an X-band radar transmitter that is widely used in ground-based surveillance and airborne radar systems due to its small antenna dimensions, fine range resolution, good coverage and robustness to weather conditions [13].

2 System Model

In the multistatic radar network, the receivers are assumed to have multiple surveillance and reference antennas operating at FM radio, DVB-T, DAB and active radar frequencies to utilise different IOs for radar sensing. The active radar transmitter and receivers are cooperative and synchronised. However, the instantaneous properties of FM radio, DVB-T and DAB signals are not known, hence the receivers also have reference antennas to acquire the reference signals from these IOs.

The multistatic radar network under consideration consists of J transmitters, I receivers and a single target for the sake of simplicity. The distance between the jth transmitter and the ith receiver (i.e., baseline) is denoted by $L_{i,j}$ and the distance between the target and the jth transmitter is denoted by T_j and the distance between the target and the ith receiver is denoted by R_i as shown in Fig. 1. The angle between the receiver and target is defined by θ_i, and the angle of the target velocity vector to the bistatic bisector is defined by $\phi_{i,j}$. Therefore, the relative velocity of the target is calculated as $V_{i,j} = V \cos \phi_{i,j}$, where V denotes the velocity of the target. Transmitters, targets and receivers are placed at (x_j, y_j, z_j), (x_t, y_t, z_t), (x_i, y_i, z_i), respectively, in a 3D coordinate system. Therefore, all of the parameters mentioned above can be calculated for all bistatic pairs using these coordinates in the simulations.

3 Monostatic Cramér-Rao Lower Bounds

It was shown that monostatic CRLBs on range and velocity estimations can be derived from the monostatic ambiguity functions of waveforms [8]. For a waveform denoted by $u(t)$, the ambiguity function is given by

$$|\Omega(\tau,\omega)| = \left| \int_{-\infty}^{+\infty} u(t)\, u^*(t-\tau)\, e^{-j2\pi\omega t} dt \right|, \qquad (1)$$

where τ and ω denote delay and Doppler frequency, respectively. The monostatic Fisher information matrix (FIM) for the delay and Doppler estimation is given by [5]

$$\mathbf{J}_M(\tau,\omega) = -2\rho\mathbf{J}_0 = -2\rho \begin{bmatrix} \frac{\partial^2\Theta(\tau,\omega)}{\partial\tau^2} & \frac{\partial^2\Theta(\tau,\omega)}{\partial\tau\partial\omega} \\ \frac{\partial^2\Theta(\tau,\omega)}{\partial\omega\partial\tau} & \frac{\partial^2\Theta(\tau,\omega)}{\partial\omega^2} \end{bmatrix}, \qquad (2)$$

where $\Theta(\tau,\omega) = |\Omega(\tau,\omega)|^2$, and ρ denotes the SNR of the received signals. $\mathbf{J}_0$ is a matrix which consists of only partial derivatives of the waveform related parameters. Matrix $\mathbf{J}_0$ will be given in the next subsections for each waveform considered in this study, i.e., $\mathbf{J}_{(LFM)}$, $\mathbf{J}_{(SFM)}$, and $\mathbf{J}_{(OFDM)}$. After computing the FIM, the monostatic CLRBs on delay and Doppler frequency can be respectively calculated by [5, 14]

$$\mathrm{CRLB}(\tau) = [\mathbf{J}_M^{-1}(\tau,\omega)]_{1,1}, \qquad (3)$$

$$\mathrm{CRLB}(\omega) = [\mathbf{J}_M^{-1}(\tau,\omega)]_{2,2}. \qquad (4)$$

3.1 LFM Waveform

LFM is widely used in radar applications due to its low-cost hardware requirements, computationally efficient processing and excellent Doppler properties [15]. The complex-valued LFM waveform is given by [5]

$$u_{LFM}(t) = \begin{cases} Ae^{j\pi kt^2} & 0 \le t \le T_p \\ 0 & else \end{cases}, \qquad (5)$$

where A denotes the amplitude of the pulse, and $k = B/T_p$ denotes the relation between the LFM pulse bandwidth, $B = f_1 - f_0$, and pulse duration T_p. The elements of FIM for delay and Doppler measurements with N LFM pulses is given by [5]

$$\mathbf{J}_{LFM} = \begin{bmatrix} \frac{-k^2\pi^2T_p^2}{3} & \frac{k\pi^2T_p^2}{3} \\ \frac{k\pi^2T_p^2}{3} & \frac{\pi^2T_R^2\left(1-N^2\right)-\pi^2T_p^2}{3} \end{bmatrix}, \qquad (6)$$

where B, T_p, T_R and N denote the bandwidth, duration of each pulse, pulse repetition interval and number of LFM pulses. The details of the FIM and CRLBs derivations of LFM waveforms can be found in [5, 8].

3.2 FM Radio Signals

As the frequency of FM radio signals varies over time, an approximate model of FM radio signals over observation

duration T is given by [12]

$$u_{SFM}(t) = \begin{cases} \frac{A}{\sqrt{T}} e^{j\beta sin(2\pi f_0 t + \phi)} & 0 \le t \le T \\ 0 & else \end{cases}, \quad (7)$$

where approximate bandwidth of the signal is expressed by Carson's bandwidth as $B_c = 2(\delta f + f_m) = 2\beta f_0$, and δf and f_m denote the peak frequency deviation and the highest frequency in the modulation signal, and ϕ denotes the phase [12]. Modified FIM expressions of FM radio signals are derived based on the approximate signal model given by (7) as [12]

$$\mathbf{J}_{SFM} = \begin{bmatrix} 4\pi^2\beta^2 f_0^2 & -(-1)^z 2\pi\beta \sin(\phi) \\ -(-1)^z 2\pi\beta \sin(\phi) & \frac{\pi^2 T^2}{3} \end{bmatrix}, \quad (8)$$

where $z = Tf_0$ is an integer and denotes the number of FM radio pulses observed.

3.3 DVB-T and DAB Signals

Both DVB-T and DAB broadcasting standards utilise coded OFDM (COFDM) scheme but with different parameters such different subcarrier spacings, bandwidths, symbol duration and cyclic-prefix duration. OFDM signals are usually processed via a root raised-cosine (RRC) filter to reduce the inter-carrier interference. Let $w(t)$ define the RRC filter response, then an OFDM waveform consisting of L symbols over N_s subcarriers is given by [16]

$$u_{OFDM}(t) = \sum_{l=0}^{L-1} \sum_{n=-N_s/2}^{N_s/2-1} A s_{n,l} e^{j2\pi n\Delta f\left(t - T_{cp} - lT_{sym}\right)} w(t - lT_{sym}). \quad (9)$$

where $s_{n,l}$ denotes the lth QAM symbol transmitted in the nth subcarrier. Moreover, Δf, T_{sym}, T_{cp} denote the OFDM subcarrier spacing, symbol duration and cyclic-prefix duration, respectively. The modified FIM and CRLBs for OFDM signals were derived in [16], where the first element of the modified FIM for an OFDM waveform consisting of L OFDM symbols is given by

$$[\mathbf{J}_{OFDM}]_{1,1} = \frac{4\pi^2 L\left(3 + \Delta f^2\left(N_s^2 - 1\right)\left(4T_{sym} - T_w\right)T_w\right)}{\left(48T_{sym} - 12T_w\right)T_w}. \quad (10)$$

Moreover, the last element of the modified FIM for an OFDM waveform consisting of L OFDM symbols can be given by

$$[\mathbf{J}_{OFDM}]_{2,2} = \frac{L}{12T_{sym} - 3T_w/4}\left[4\pi^2 L^2 T_{sym}^3 - \pi^2\left(L^2 + 2\right)T_{sym}^2 T_w - \left(\pi^2 - 6\right)T_w^3 + 12\left(\pi^2 - 8\right)T_{sym}T_w^2\right]. \quad (11)$$

The other two elements of FIM for OFDM signals are given as $[\mathbf{J}_{OFDM}]_{1,2} = [\mathbf{J}_{OFDM}]_{2,1} = 0$ [16].

4 Bistatic Cramér-Rao Lower Bounds

The bistatic CRLBs on range and velocity estimations were derived in [5], which also shows that bistatic CRLBs can be decoupled into geometry-related and waveform-related parameters. The bistatic FIM with regards to target range R_i from receiver and target relative velocity $V_{i,j}$ is given by [5]

$$\mathbf{J}_B(R_i, V_{i,j}) = -2\rho_{i,j}\begin{bmatrix} \frac{\partial^2\Theta\left(R_i,V_{i,j}\right)}{\partial R_i^2} & \frac{\partial^2\Theta\left(R_i,V_{i,j}\right)}{\partial R_i \partial V_{i,j}} \\ \frac{\partial^2\Theta\left(R_i,V_{i,j}\right)}{\partial V_{i,j}\partial R_i} & \frac{\partial^2\Theta\left(R_i,V_{i,j}\right)}{\partial V_{i,j}^2} \end{bmatrix}, \quad (12)$$

where partial derivatives of $\Theta(R_i, V_{i,j})$ with respect to target range R_i and target relative velocity $V_{i,j}$ can be calculated as

$$\frac{\partial^2\Theta(R_i, V_{i,j})}{\partial R_i^2} = [\mathbf{J}_0]_{1,1}\left(\frac{\partial\tau}{\partial R_i}\right)^2 + 2[\mathbf{J}_0]_{1,2}\frac{\partial\tau}{\partial R_i}\frac{\partial\omega}{\partial R_i} + [\mathbf{J}_0]_{2,2}\left(\frac{\partial\omega}{\partial R_i}\right)^2, \quad (13)$$

$$\frac{\partial^2\Theta(R_i, V_{i,j})}{\partial V_{i,j}^2} = [\mathbf{J}_0]_{2,2}\left(\frac{\partial\omega}{\partial V_{i,j}}\right)^2, \quad (14)$$

$$\frac{\partial^2\Theta(R_i, V_{i,j})}{\partial R_i \partial V_{i,j}} = [\mathbf{J}_0]_{1,2}\frac{\partial\tau}{\partial R_i}\frac{\partial\omega}{\partial V_{i,j}} + [\mathbf{J}_0]_{2,2}\frac{\partial\omega}{\partial R_i}\frac{\partial\omega}{\partial V_{i,j}}, \quad (15)$$

where $\mathbf{J}_0$ denotes the FIM resulting from only waveform related parameters as given for LFM, FM and OFDM waveforms in the previous section. This demonstrates that the bistatic CRLBs of the Tx-Rx pairs can be decoupled into waveform and geometry related parameters, and this reduces the computational complexity as waveform parameters are generally constant while the bistatic geometry varies over the time.

5 Simulations and Numerical Results

In the simulated multistatic networks, active radar transmitter (LFM), DVB-T, DAB and FM radio broadcasting stations, and two multi-band receivers are placed in various locations in the area of interest, represented by a 3D coordinate system. For the sake of simplicity, only a single target is considered. The altitude of the target is 400 m, and the height of FM radio, DVB-T, DAB transmitters and receiver antennas are considered as 100 m, 20 m, 20 m and 5 m, respectively. Other transmitter and waveform parameters used in the simulations are given in Table 1. Each Tx-Rx pair with the target creates a bistatic geometry of which CRLBs are computed in the simulations using the model explained in the previous sections. The target radar cross-section (RCS) is assumed to be 0 dBm^2.

An X-band radar transmitter emitting LFM waveforms with 50 MHz bandwidth at 9.4 GHz carrier frequency is considered for the active radar operations. Since the antenna size is very

Table 1 Transmitter and waveform parameters

Waveform	Modulation	f_c	Bandwidth	Pulse/Duration	Power	Antenna Gain (G_tG_r)
FM Radio	SFM	100 MHz	75 kHz ($f_0 = 15$ kHz, $\beta = 5$)	100 ms observation	20 kW	4.3 dBi
DVB-T 8K	COFDM	500 MHz	7.61 MHz (6816×1116 Hz)	64 symbols in 57.3 ms	5 kW	4.3 dBi
DAB	COFDM	150 MHz	1.536 MHz (768×2000 Hz)	64 symbols in 40 ms	5 kW	4.3 dBi
Radar Chirp	LFM	9.4 GHz	50 MHz	64 pulses in 25.6 ms	10 kW	50 dBi

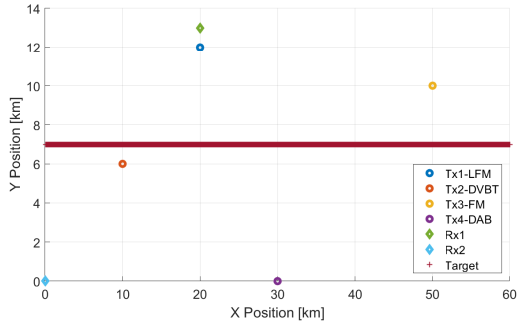

Fig. 2. Scenario 1.

small in X-band frequencies, an antenna array with a gain of 25 dBi at both transmitter and receiver are assumed for active sensing, resulting in 50 dBi total gain while dipole antennas with a gain of 2.15 dBi at both ends are considered for IO signals to provide an omnidirectional coverage. An LFM waveform consisting of 64 pulses with $T_p = 200$ μs pulse duration and $T_r = 400$ μs pulse repetition interval are considered for active sensing while 100 ms signal observation is used for passive sensing with FM signals and 64 OFDM symbols are utilised for DVB-T and DAB signals.

Fig. 2 illustrates the first scenario considered for the multistatic radar network, where a single target moves forward along the x-axis starting from 0 km position. It is worth noting that Tx1 and Rx1 are close to each other, thus, they create a quasi monostatic active radar system. The bistatic root CRLBs (RCRLBs, $\sqrt{CRLB}$), on the range and velocity estimations of this scenario are given by Fig. 3 and Fig. 4, respectively. Taking into account the bistatic geometries between the Tx-Rx pairs presented in Fig. 2, the impact of the bistatic geometry is clearly observed in Fig. 3 and Fig. 4 such that RCRLBs rapidly increase when the target approaching or crossing the baseline of the Tx-Rx pairs, resulting higher range and velocity estimation errors. Therefore, as the target moves forward, different Tx-Rx pairs become more desirable for estimating the target parameters. For instance, when the target is at around 10 km x-position, the DVB-T transmitter provides a better range and velocity estimations than the active radar transmitter. When the target is far away, FM signals may provide more accurate velocity estimations as shown in Fig. 4.

In the second scenario illustrated in Fig. 5, Rx2 is moved to (x=40, y=3) km location and the target follows a diagonal trajectory. The change of the RCRLBs with regard to bistatic geometry is also observed in this scenario as the target crosses baseline of Tx-Rx pairs while moving. For instance, a significant peak in the RCRLBs of Tx3-Rx1 pair is observed as

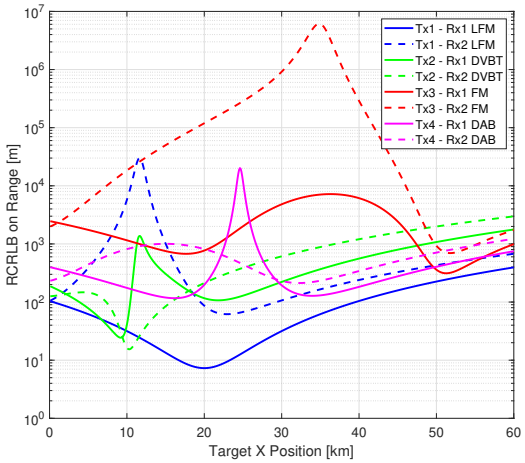

Fig. 3. RCRLB on the range in scenario 1.

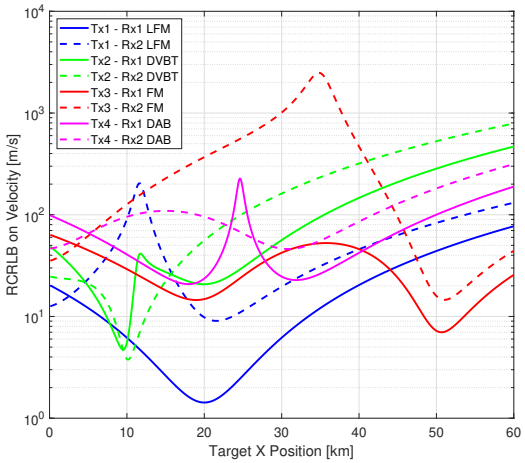

Fig. 4. RCRLB on the velocity in scenario 1.

the target approaches the baseline of this pair. Fig. 6 indicates that Tx2-Rx1 (DVB-T) and Tx4-Rx2 (DAB) pairs may provide sufficient range estimations in different parts of the target trajectory as they achieve the lowest RCRLBs on range after the active radar pairs, depending on the target location. For instance, when the target is around 50 km x-position, Tx3-Rx2 (FM) provides the best range estimation among all pairs. A similar situation can also be observed in the case of velocity estimation as shown in Fig. 7. These results show that an active radar transmitter can be supported by passive radar sensing opportunities to improve the accuracy of range

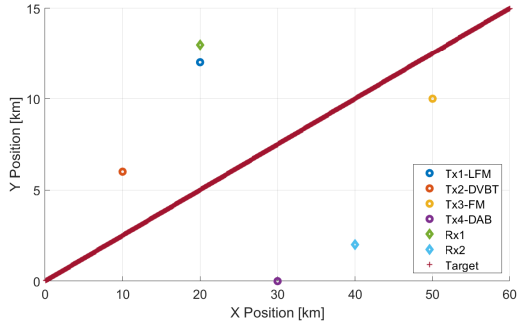

Fig. 5. Scenario 2.

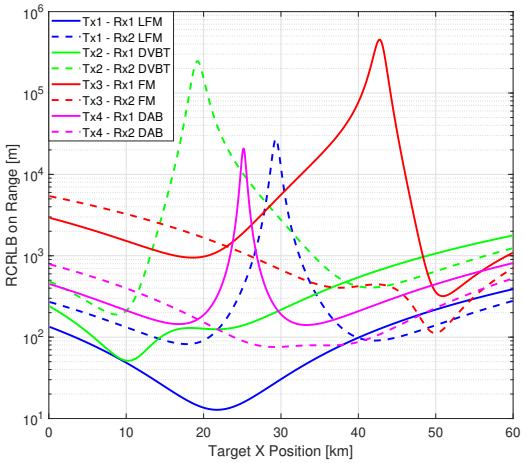

Fig. 6. RCRLB on the range in scenario 2.

and velocity estimations. Moreover, it is possible to switch off the active transmitter when the passive sensing provides sufficiently accurate estimations.

Fig. 8 and Fig. 9 present the average RCRLBs on range and velocity of all pairs, and also combination of all of them and combination of only passive sensing pairs in these scenarios. Combination of all pairs is obtained by selecting the pairs that deliver the best estimation accuracy for a given target location. It should be noted that the maximum RCRLBs are limited to 10^3 for both range and velocity estimations while calculating the average RCRLBs presented in these figures to reduce the impact of the outliers on the averages. It can be seen that active pairs provides the overall best average range and velocity estimations in both scenarios. However, in some target locations, one or two passive sensing pairs may provide better estimation than active sensing when the active sensing is degraded by the bistatic geometry or low SNR.

While average expected estimation errors are relatively high for each passive sensing pair, however, by combining only passive pairs provided reasonable RCRLBs in both scenarios as indicated by 'Combined-Passive' in Fig. 8 and Fig. 9. This demonstrates the importance of having multi-band multi-waveform receivers and utilising two or more IOs in the area of interest to achieve a desirable target parameter estimation

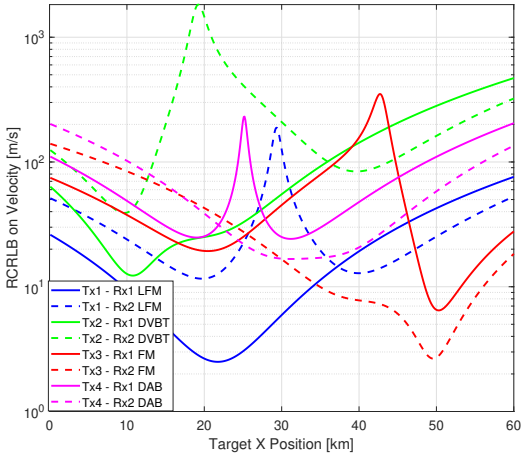

Fig. 7. RCRLB on the velocity in scenario 2.

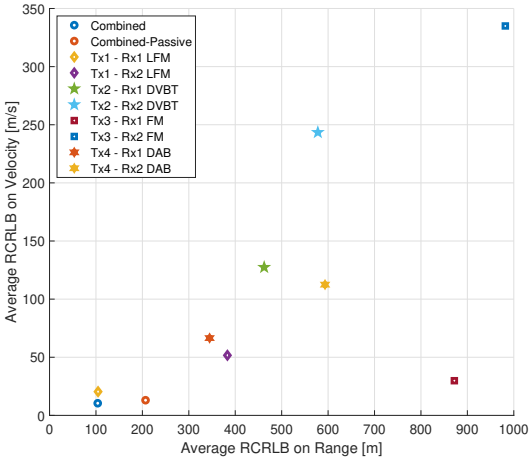

Fig. 8. Average RCRLBs on velocity and range in scenario 1.

accuracy. Based on the information obtained from these simulations, the radar can switch between the waveforms and even can switch off emitting LFM waveform to perform in entirely passive mode when it is necessary. Moreover, in the case of jamming, the radar can decide using another waveform which is not jammed since the carrier frequencies of the waveforms are significantly different.

This modelling and analysis can be performed for real multi-band multistatic radar networks as the locations of broadcasting stations are fixed and known, and the locations of the radar transmitter and receivers are known by the radar. Based on this information, the radar system will be able to create a lookup table that contains the information of the best pairs for the different locations in the area of interest for passive sensing, therefore, the radar can choose the best Tx-Rx pairs that provide the lowest CRLBs to obtain the best possible range and velocity estimations of the target.

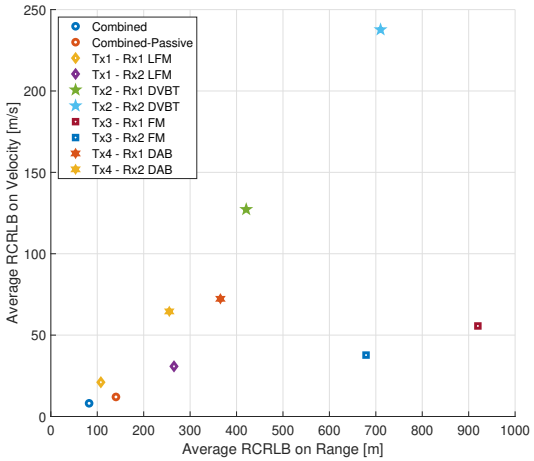

Fig. 9. Average RCRLBs on velocity and range in scenario 2.

6 Conclusion

In this study, we have investigated multi-band hybrid multi-static radar networks that utilise an active radar transmitter and also DVB-T, DAB and FM radio signals to improve the range and velocity estimations. As a performance metric, the bistatic CRLBs of Tx-Rx pairs are used, which determine theoretical lower bounds of estimation errors. The results have shown that bistatic geometry significantly impacts the range and velocity estimations, hence relying on only a single transmitter may result in some blind areas in the radar network, especially around the baseline of the Tx-Rx pair. Moreover, the results shown would vary with new geometries, however, the importance shown here is that different waveforms can provide better estimations at different points of a scenario. Knowledge of this is important for future cognitive/intelligent radar systems which may be looking to decide what signal to use to perform their sensing. The analysis shown here gives an insight into the potential advantages of considering other IOs available in the area of interest in addition to radar transmitters. A fused multi-band multistatic sensing system brings significant benefits and also provides robustness to any possible jamming that is generally designed to corrupt active radar waveform, hence, active sensing Tx-Rx pairs. Consequently, radar fusion systems should be the future direction of intelligent RF sensor networks.

Acknowledgement

This work was supported by the University Defence Research Collaboration (UDRC) and was jointly funded by the Engineering and Physical Sciences Research Council (EPSRC) and the Defence Science and Technology Laboratory (Dstl).

7 References

[1] H. D. Griffiths and C. J. Baker, *An introduction to passive radar*. Artech House, 2017.

[2] H. Kuschel, D. Cristallini, and K. E. Olsen, "Tutorial: Passive radar tutorial," *IEEE Aerospace and Electronic Systems Magazine*, vol. 34, pp. 2–19, Feb 2019.

[3] P. Stinco, M. Greco, F. Gini, and M. Rangaswamy, "Ambiguity function and Cramér–Rao bounds for universal mobile telecommunications system-based passive coherent location systems," *IET Radar, Sonar & Navigation*, vol. 6, no. 7, pp. 668–678, 2012.

[4] A. S. Evers, *Evaluation and application of LTE, DVB, and DAB signals of opportunity for passive bistatic SAR imaging*. PhD thesis, Wright State University, 2014.

[5] M. S. Greco, P. Stinco, F. Gini, and A. Farina, "Cramer-Rao bounds and selection of bistatic channels for multistatic radar systems," *IEEE Transactions on Aerospace and Electronic Systems*, vol. 47, pp. 2934–2948, October 2011.

[6] Q. Chen, X. Zhang, Q. Yang, L. Ye, and M. Zhao, "Performance bound for joint multiple parameter target estimation in sparse stepped-frequency radar: A comparison analysis," *Sensors*, vol. 19, no. 9, 2019.

[7] H. Godrich, A. M. Haimovich, and R. S. Blum, "Target localization accuracy gain in MIMO radar-based systems," *IEEE Transactions on Information Theory*, vol. 56, pp. 2783–2803, June 2010.

[8] A. Dogandzic and A. Nehorai, "Cramer-Rao bounds for estimating range, velocity, and direction with an active array," *IEEE Transactions on Signal Processing*, vol. 49, pp. 1122–1137, June 2001.

[9] M. Edrich, A. Schroeder, and F. Meyer, "Design and performance evaluation of a mature FM/DAB/DVB-T multi-illuminator passive radar system," *IET Radar, Sonar & Navigation*, vol. 8, no. 2, pp. 114–122, 2014.

[10] S. Paine, F. Schonken, M. Malape, D. W. O'Hagan, J. Swart, F. Louw, and M. Setsubi, "Multi band FM and DVB-T2 passive radar demonstrator," in *19th International Radar Symposium (IRS)*, pp. 1–10, June 2018.

[11] D. Dhulashia, M. Temiz, and M. A. Ritchie, "Jamming effects on hybrid multistatic radar network range and velocity estimation errors," *IEEE Access*, vol. 10, pp. 27736–27749, 2022.

[12] M. Greco, P. Stinco, F. Gini, A. Farina, and M. Rangaswamy, "Cramér-Rao bounds and Tx-Rx selection in a multistatic radar scenario," in *2010 IEEE Radar Conference*, pp. 1371–1376, May 2010.

[13] S. Saponara and B. Neri, "Design of compact and low-power X-band radar for mobility surveillance applications," *Computers & Electrical Engineering*, vol. 56, pp. 46–63, 2016.

[14] T. Abatzoglou and G. Gheen, "Range, radial velocity, and acceleration MLE using radar LFM pulse train," *IEEE Transactions on Aerospace and Electronic Systems*, vol. 34, pp. 1070–1083, Oct 1998.

[15] S. D. Blunt and E. L. Mokole, "Overview of radar waveform diversity," *IEEE Aerospace and Electronic Systems Magazine*, vol. 31, pp. 2–42, November 2016.

[16] A. Filip and D. Shutin, "Cramér–Rao bounds for L-band digital aeronautical communication system type 1 based passive multiple-input multiple-output radar," *IET Radar, Sonar & Navigation*, vol. 10, no. 2, pp. 348–358, 2016.